Finite-Difference Calculation of Hypersonic Wakes

SEYMOUR L. ZEIBERG* AND GARY D. BLEICH†
General Applied Science Laboratories, Inc., Westbury, N. Y.

A finite-difference method is used to solve the system of equations governing the hypersonic air wake with nonequilibrium chemistry; both laminar and turbulent transports are considered. Numerical results for laminar flow are compared with results of an integral method. Additional calculations for turbulent flow are presented to show some effects of the oxygen-electron attachment process in the far wake, and of the choice of the model of turbulent diffusivity.

Nomenclature

C_P = specific heat
D = vehicle base diameter
L = Lewis number
h = enthalpy
h^0 = enthalpy of formation
P = pressure
R_b = vehicle base radius
T = temperature
U = X component of velocity
U = velocity defect
V = Y component of velocity
$\dot{w}_i$ = net rate of generation of species i
X = streamwise coordinate
Y = radial coordinate
α = mass fraction
δ_U = velocity radius
η = density transformed radial coordinate
σ = Prandtl number
μ = viscosity
ρ = density
Ψ = stream function

Subscripts

0 = evaluated on wake axis $Y = \Psi = 0$
e = evaluated at edge of wake, or freestream
i = refers to species i

Superscript

$\overline{(\ )}$ = mass-averaged quantity

I. Introduction

THE problems associated with the detection and tracking of vehicles re-entering the earth's atmosphere have provided the stimulus for the study of observables associated with wakes of hypersonic re-entry vehicles; Refs. 1–20 (for example) contain descriptions and analyses of the numerous and varied aspects of re-entry wake phenomena. However, the forementioned works are all based upon approximate methods of analysis. The techniques that have been used are direct applications of classical integral methods[21] with some modifications to include, for example, nonequilibrium air chemistry,[4, 8, 11, 18–20] a vortical, inviscid external flow into which the viscous wake grows,[2, 11, 15, 16, 19, 20] the effect of vehicle attitude oscillations,[6, 7] and the effect of a varying freestream density along the wake.[6, 17] The integral-strip method[22, 23] has also been applied to the hypersonic wake.[13, 18]

In order to describe flow details with precision throughout the flow field, to allow matching of specific initial conditions, and to allow nonsimilar flow behavior, it is necessary to abandon the conventional integral method and employ more refined methods of analysis. The use of the integral-strip method affords the opportunity for such improvement; however, a large number of strips is required for marked improvement, and then the problem approaches a finite-difference calculation. The latter technique is the one employed herein. The finite-difference method represents an exact solution of the governing equations for arbitrarily prescribed initial and boundary conditions. Thus, in addition to being a valuable computational facility, it also serves the function of a reference from which approximate methods of analysis may be evaluated.

Finite-difference techniques have been applied to viscous flows by many investigators; Refs. 24–31 present results of boundary-layer studies, whereas Refs. 32 and 33 show results for jet flows. The latter includes finite-rate chemical reactions for hydrogen and carbon monoxide combustion. References 24–26 contain detailed discussions of the application of finite-difference methods to the boundary-layer equations.

The present work deals with the axisymmetric hypersonic air wake including finite-rate dissociation and recombination processes for the representative air species; both laminar and turbulent flows are considered. The following section describes the general formulation of the analysis. Subsequent sections present numerical comparisons of the method with an integral method[8] and a comparison of slender-body turbulent wakes calculated with different turbulent diffusivity models; the latter also indicate some laminar-turbulent transition effects and oxygen-electron attachment effects.

II. General Formulation

The flow under analysis here is the region downstream of the wake neck (Fig. 1); it is assumed that the boundary-layer equations apply, and that the flow properties of the "outer wake" may be approximated by the freestream properties. Thus, the wake grows into a uniform external flow, and thereby the analysis is restricted to wakes behind slender configurations or to the far downstream regions behind vehicles with large nose-bluntness. The generalization of the present work to include the "swallowing" of a vortical, inviscid, reacting outer wake is in preparation. Webb and Hromas[20] have studied such a flow by an extension of the Lees-Hromas integral method analysis.[2]

Presented as Preprint 63-448 at the AIAA Conference on Physics of Entry into Planetary Atmospheres, Cambridge, Mass., August 26–28, 1963; revision received April 8, 1964. The work reported here was performed under Contract NOrd 18053 for the Special Projects Office, Bureau of Naval Weapons, Department of the Navy, and under subcontract to Lincoln Laboratory, a center for research operated by Massachusetts Institute of Technology with support from the U. S. Advanced Research Projects Agency.

* Project Scientist. Member AIAA.
† Engineer. Associate Member AIAA.

With X, Y being the physical streamwise and radial axisymmetric coordinates, the governing equations[34] are transformed to the Von Mises coordinates S, Ψ defined by

$$S = X \tag{1}$$

$$\Psi(\partial\Psi/\partial Y) = \rho UY \qquad \Psi(\partial\Psi/\partial X) = -\rho VY \tag{2}$$

The use of the stream function satisfies the over-all continuity equation, whereas the other pertinent conservation laws become the following:

Momentum

$$\frac{\partial U}{\partial S} = -\frac{1}{\rho U}\frac{dp}{dX} + \frac{1}{\Psi}\frac{1}{\partial\Psi}\left[\frac{\mu\rho UY^2}{\Psi}\frac{\partial U}{\partial\Psi}\right] \tag{3}$$

Energy

$$\bar{C}_p\frac{\partial T}{\partial S} = \frac{1}{\rho}\frac{dp}{dX} + \frac{1}{\Psi}\frac{1}{\partial\Psi}\left[\left(\frac{\bar{C}_p}{\sigma}\right)\frac{\mu\rho UY^2}{\Psi}\frac{\partial T}{\partial\Psi}\right] + \frac{\mu\rho UY^2}{\Psi^2}\left[\left(\frac{\partial U}{\partial\Psi}\right)^2 + \left(\frac{L}{\sigma}\right)\frac{\partial T}{\partial\Psi}\sum_i C_{pi}\frac{\partial\alpha_i}{\partial\Psi}\right] - \frac{1}{U}\sum_i h_i\dot{w}_i \tag{4}$$

Species continuity

$$\frac{\partial\alpha_i}{\partial X} = \frac{1}{\Psi}\frac{\partial}{\partial\Psi}\left[\left(\frac{L}{\sigma}\right)\frac{\mu\rho UY^2}{\Psi}\frac{\partial\alpha_i}{\partial\Psi}\right] + \frac{\dot{w}_i}{U} \tag{5}$$

A streamwise pressure gradient (assumed to be specified) is included to allow the possibility of a radially uniform but streamwise varying external flow.

The boundary conditions are those of symmetry at $\Psi = 0$ and matching to the freestream as $\Psi \to \infty$. The initial conditions at $S = 0$ are specified as functions of Ψ. In the case of turbulent flow, the governing equations just listed are assumed to describe the temporal mean flow properties.[34]

Equations (4) and (5) are written with the assumption that the binary diffusion laws are applicable to mass diffusion in the dissociated-air laminar wake. Some justification of this assumption is discussed in Refs. 8 and 35. Also, the use of coupled, multicomponent formalism for the mass diffusion is limited by the paucity of data for the pertinent binary diffusion coefficients. For turbulent flows, it is assumed that the Reynolds analogy for mass, momentum, and energy transport is valid.

For laminar flow, the transport parameters (Lewis number L and Prandtl number σ) and the viscosity are well defined. (In the present work, the Sutherland law is used for the latter.) Arbitrary values of L and σ are allowed in the analysis. However, for turbulent flow, L and σ must be interpreted as their operationally defined turbulent counterparts; values of unity have been used. The form of the turbulent viscosity is discussed in detail in a later section.

The air chemistry employed herein assumes vibrational equilibrium and includes the species O_2, O, N_2, N, NO, NO^+, O_2^-, and e^-. These species are active in the following reactions:

$$C + N_2 \rightleftarrows 2N + C \tag{6a}$$

$$C + O_2 \rightleftarrows 2O + C \tag{6b}$$

$$C + NO \rightleftarrows N + O + C \tag{6c}$$

$$NO + O \rightleftarrows N + O_2 \tag{6d}$$

$$N_2 + O \rightleftarrows NO + N \tag{6e}$$

$$N_2 + O_2 \rightleftarrows 2NO \tag{6f}$$

$$N + O \rightleftarrows NO^+ + e^- \tag{6g}$$

$$C + NO \rightleftarrows NO^+ + e^- + C \tag{6h}$$

$$2O_2 + e^- \rightleftarrows O_2^- + O_2 \tag{6i}$$

$$NO^+ + O_2^- \rightleftarrows NO + O_2 \tag{6j}$$

in which C is a catalyst.

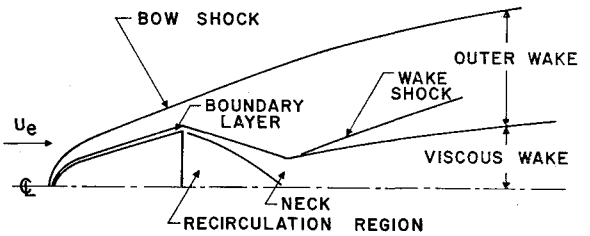

Fig. 1 Schematic sketch of flow field.

The reaction rates used for the preceding reactions are those quoted in Refs. 36–38. In the absence of data concerning reaction rates in turbulent flows, the laminar rates are assumed to apply to turbulent flows also. This assumption must be regarded as being imposed by the state of the art and does not reflect the opinion that the macroscopic inhomgeneity of the turbulent flow does not influence chemical reactions.

The system of governing equations is completed by specifying the equation of state, the $h - T - \alpha_i$ relation, overall mass conservation, charge conservation, and the phenomenological rate equations for the $\dot{w}_i$. The details of the formulation of the rate equations may be found in standard texts (e.g., Ref. 41). The state and conservation equations are

$$P = (\rho RT)/[\Sigma_i(\alpha_i/M_i)] \tag{7a}$$

$$h = \Sigma_i\,\alpha_i h_i = \Sigma_i\,\alpha_i[C_{pi}T + h_i^0] \tag{7b}$$

$$\Sigma_i\,\alpha_i = 1 \tag{7c}$$

$$\frac{\alpha_{NO^+}}{M_{NO^+}} = \frac{\alpha_{e^-}}{M_{e^-}} + \frac{\alpha_{O_2^-}}{M_{O_2^-}} \tag{7d}$$

Equations (7c) and (7d) allow consideration of only $i - 2$ species continuity equations, rather than i equations. However, in the present work, all i equations are calculated, and (7c) and (7d) are used as check sums in order to provide some of the information from which numerical accuracy may be judged.

The finite-difference formulation of the governing conservation equations is accomplished by employing the following explicit difference relations[39, 40] for a typical variable F:

$$\frac{\partial F}{\partial S} = \frac{F(S + \Delta S, \Psi) - F(S, \Psi)}{\Delta S} \tag{8a}$$

$$\frac{\partial F}{\partial\Psi} = \frac{F(S, \Psi + \Delta\Psi) - F(S, \Psi - \Delta\Psi)}{2\Delta\Psi} \tag{8b}$$

$$\frac{\partial}{\partial\Psi}\left[a\frac{\partial F}{\partial\Psi}\right] = \frac{a(S, \Psi + \frac{1}{2}\Delta\Psi)[F(S, \Psi + \Delta\Psi) - F(S, \Psi)]}{(\Delta\Psi)^2} - \frac{a(S, \Psi - \frac{1}{2}\Delta\Psi)[F(S, \Psi) - F(S, \Psi - \Delta\Psi)]}{(\Delta\Psi)^2} \tag{8c}$$

in which

$$a(S, \Psi \pm \tfrac{1}{2}\Delta\Psi) = \tfrac{1}{2}[a(S, \Psi) + a(S, \Psi \pm \Delta\Psi)] \tag{8d}$$

Equations (3–5) are "numerically singular" on the wake axis ($\Psi = 0$). However, alternate forms of these equations suitable for computation on $\Psi = 0$ are readily derived with the use of l'Hôspital's rule and the axis symmetry conditions, i.e., at $\Psi = 0$,

$$\frac{\partial U}{\partial\Psi} = \frac{\partial T}{\partial\Psi} = \frac{\partial\alpha_i}{\partial\Psi} = 0 \tag{9a}$$

Numerically, Eqs. (9a) are expressed as

$$f(S, \Delta\Psi) = f(S, -\Delta\Psi) \tag{9b}$$

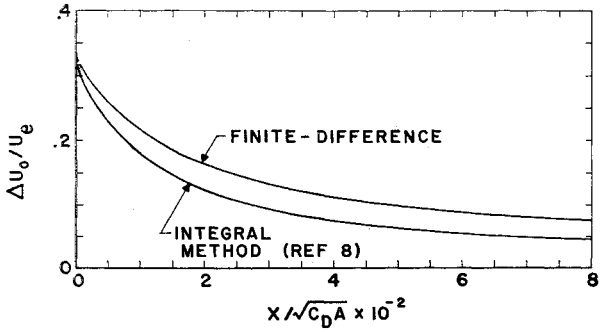

Fig. 2 Axis velocity defect; laminar wake of a hemisphere-cylinder (250 kft, 18.5 kft/sec). Comparison with integral method.

The governing conservation equations are parabolic, and thus, the use of the explicit finite-difference method subjects the system of equations to stability conditions that govern the permissible relative grid dimensions (e.g., see Refs. 39 and 40). Furthermore, in the present nonlinear problem, it is not possible to determine by analytical means the precise stability requirements. It is possible, however, to provide estimates based on the application of linear theory. These estimates, plus numerous trial calculations, provided the basis for the determination of the stability conditions pertinent to the present problem. The analytical estimate is given by

$$\Delta S \leqq (\sigma/\mu L)_0[(\Delta\Psi)^2/4] \tag{10}$$

The choice of the explicit method and its stability problems over the "always-stable" implicit method is based on the fact that the step sizes required for accurate calculation of the more rapid chemical reactions (e.g., near equilibrium) are generally much smaller than the estimated explicit stability limit. Therefore, no advantage would be gained by using the implicit method.

In general, the resulting difference equations are of the form

$$F(S + \Delta S, \Psi) = A(S, \Psi) + B(S, \Psi - \Delta\Psi) + C(S, \Psi + \Delta\Psi) + D(S) \tag{11}$$

in which F is either U, T, or the α_i, and the functions A, B, C, and D depend on the equation being considered. The details of the difference equations, the chemical production terms ($\dot{w}$), and the rate constants and thermodynamic data are not shown here because of space limitations; this information is available in Ref. 42.

Starting with specified initial conditions, the calculation marches forward with the streamwise step size controlled automatically. The step size may be doubled or halved, depending upon the relative accuracy of the results of a parallel sequence of forward steps both with the "current" step size and with a step size of twice this value.

The radial mesh grows in order to satisfy the "zero-slope" boundary condition at "infinity," i.e., as $\Psi \to \infty$,

$$\partial U/\partial\Psi,\ \partial T/\partial\Psi,\ \partial\alpha_i/\partial\Psi \to 0 \tag{12}$$

whereas U, T, and α_i approach their respective freestream values. This boundary condition is satisfied by using a large enough number of radial grid points (the outermost being at freestream conditions) to insure negligible gradients at the outer edge.

In order to provide some information concerning numerical accuracy of a particular calculation, various quantities are computed. The integrated forms of the conservation laws, charge conservation, summation of mass fractions, and conservation of elements are checked at the appropriate places in the calculation.

Numerous calculations of a diagnostic nature have been performed and are reported in Ref. 42. Incompressible flows for which asymptotic solutions are available[21] and flows for which Crocco integrals exist were studied. In these cases, the known solutions or relations between solutions for different flow properties were reproduced. However, rather than presenting these "debugging" results here, some applications of the program are presented.

The next section presents a comparison of finite-difference and integral method[8] calculations for a laminar flow. Following this, the influence of the turbulent diffusivity model on a turbulent wake is examined. Included in the latter calculations are some indications of laminar-turbulent transition effects and oxygen-electron attachment effects.

III. Comparison with an Integral Method

An important function of a large-scale computational effort, such as the present work, is to use it as a reference according to which approximate analytical methods may be evaluated. Hence, a comparison with an integral method solution of the laminar hypersonic wake is presented here.

The integral method being used for the comparison is the one reported by Bloom and Steiger.[8] For the sake of clarification, the following is noted: the integral method solves

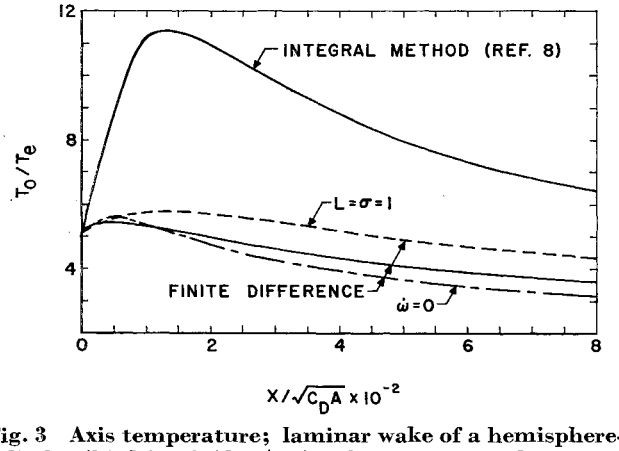

Fig. 3 Axis temperature; laminar wake of a hemisphere-cylinder (250 kft, 18.5 kft/sec). Comparison with integral method.

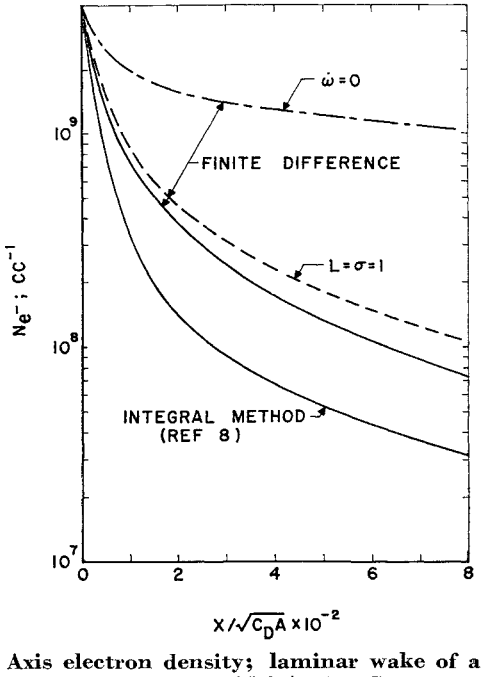

Fig. 4 Axis electron density; laminar wake of a hemisphere-cylinder (250 kft, 18.5 kft/sec). Comparison with integral method.

the integral energy and momentum equations, and the axis equations for energy, momentum, and species conservation. These equations are solved for wake radius (the same for all flow variables), axis values of velocity, stagnation enthalpy, and mass fractions, and the axis value of the curvature of the stagnation enthalpy profile. The profiles are assumed to be fourth-degree polynominals for velocity and mass fractions (a Crocco relation) and a fifth-degree polynomial for stagnation enthalpy.

The case of the laminar far wake of a hemisphere-cylinder ($L/D = 3$, $C_DA = 1$ ft^2) having a velocity of 18,500 fps at 250 kft is considered for the comparison.

Identical initial conditions were used for both the integral and the finite-difference calculations. These were obtained by computing the inviscid, reacting surface streamline along a hemisphere-cylinder shape until the pressure decreased to the freestream value. The conditions at this point were assumed to apply to the wake axis[1]; radial distributions were determined from the integral method profiles. Constant stagnation enthalpy (equal to freestream value) was used. Nominal values of $L = 1.45$ and $\sigma = 0.71$ were used in the wake (unless otherwise noted); oxygen-electron attachment was not included.

Comparisons of axis velocity defect, axis temperature, and axis electron density are shown in Figs. 2–4. Also shown in Figs. 3 and 4 are results for frozen chemistry ($\dot{w}_i = 0$) and results for Lewis and Prandtl numbers equal to unity ($L = \sigma = 1$).

Figure 5 shows the streamwise variation of the profile curvature parameter

$$[1/(Q_e - Q_0)](\partial^2 Q/\partial\eta^2)_0$$

in which Q is a flow variable, and

$$\eta^2 = 2\int_0^y \frac{\rho}{\rho_e}\, y dy$$

i.e., the density-transformed radial coordinate.

The data clearly show that some of the integral method predictions are in serious error for this case. However, the integral method does correctly predict the general behavior of the flow variables; experience with such a "one-strip" integral method has shown that generally the variables that are sensitive to the nonequilibrium chemistry may be subject to large errors, whereas other variables (e.g., velocity) are predicted reasonably well.

The effects of Lewis and Prandtl numbers of unity are seen to be modest for the case shown here. Also of interest is that the present $L = \sigma$ effects upon temperature contradict the effects predicted by the integral method; in the latter,[8] the temperature for $L = \sigma = 1$ is always lower than that for $L = 1.45$, $\sigma = 0.71$. This has been found to be a result of off-axis chemical activity and the nonexistence of a Crocco relation (as assumed for the integral method) between velocity and mass fractions.[42]

The frozen-flow calculation serves the purpose of pointing out the fact that, although the temperature and velocity‡ may be accurately predicted by the frozen chemistry at this high altitude, the electron density is clearly not frozen. Additionally, it is noteworthy that the frozen-flow temperature may be higher than the temperature in the finite-rate-reaction case. In the present case this occurs for $X/(C_DA)^{1/2} < 100$ and is mostly due to energy being absorbed by the formation of NO in the finite-rate case and to the differences in the species profiles of the two flows. The profile curvature parameter shown in Fig. 5 indicates (for the finite-rate case) some of the differences that exist between diffusion characteristics of different species and between the velocity and

‡ The frozen-flow velocity, as in the $L = \sigma = 1$ case, is within a few percent of the finite-rate value.

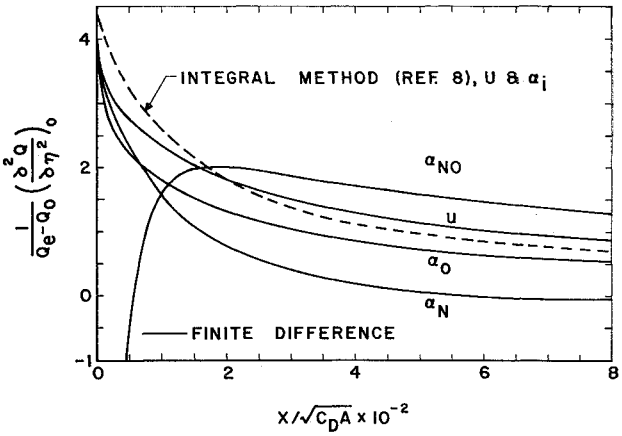

Fig. 5 Axis profile curvature parameter; laminar wake of a hemisphere-cylinder (250 kft, 18.5 kft/sec). Comparison with integral method.

the various species.§ It is not until $X/(C_DA)^{1/2} \simeq 300$ that all of the curves become essentially parallel, thereby indicating a form of similarity between profiles. This profile similarity is based upon a different wake radius for each flow variable; then the parameter

$$[1/(Q_e - Q_0)](\partial^2 Q/\partial N_Q^2)_0 = \text{const}$$

in which $N_Q = \eta/\delta_Q$, where δ_Q is the transformed wake radius associated with the variable Q. The curvature parameter for the integral method is also shown in Fig. 5; it is the same for velocity and all mass fractions, as a result of the assumption of a Crocco relation between velocity and species mass fractions.

IV. Turbulent Wake Calculations

The current state of turbulent flow analysis requires that the "laminar-type" equations be used in conjunction with an operationally defined turbulent viscosity, i.e., the eddy diffusivity concept. In connection with high-speed jet and wake analysis, several models have been proposed. In the present section these diffusivity models are tabulated, and turbulent, hypersonic wake calculations using the various models are presented. Also, some indications of the effect of laminar-turbulent transitions are shown; the transition criterion is based upon the correlations presented by Pallone et al.[13]

The turbulent viscosity models considered herein are the following:

Model 1

$$\mu = K\delta'\rho_0(U_e - U_0) \tag{13}$$

Model 2

$$\mu = Kb_{1/2}[(\rho U)_e - (\rho U)_0] \tag{14}$$

Model 3

$$\mu = K\delta'(U_e - U_0)(\rho_e^2/\rho)(\eta/Y)^2 \tag{15}$$

Model 4

$$\mu = K\delta'\rho_e(U_e - U_0) \tag{16}$$

In the foregoing, δ' is the density transformed wake radius; in the present work, this is taken as the value of η at which

$$(U_e - U)/(U_e - U_0) = 0.01$$

§ Although it is not obvious from Fig. 4, the curvature parameter for α_{NO} is identical to all others at $X/C_DA^{1/2} = 0$; for $X > 0$, the α_{NO} develops an off-axis peak due to off-axis chemistry.

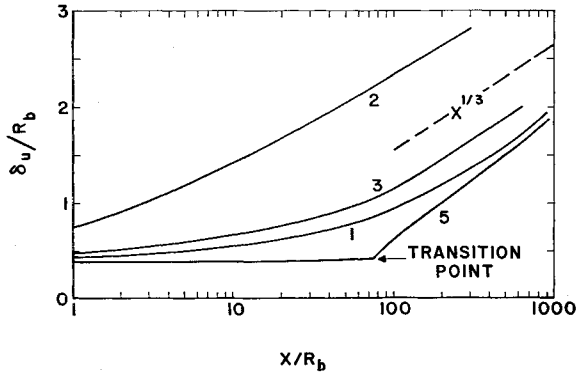

Fig. 6 Variation of velocity radius (10° cone, 120 kft, R_b = 1 ft). Turbulent and transition wakes.

The parameter $b_{1/2}$ in model 2 is a physical half-width for the quantity (ρU), i.e., it is the value of Y at which

$$\rho U = \tfrac{1}{2}[(\rho U)_e + (\rho U)_0]$$

The origins of these models are indicated below.

The analysis of low-speed turbulent free-mixing problems in flow regimes where similarity exists has led to an expression of the form $Kl\Delta U$ for the eddy diffusivity[21,43]; here l is a reference length that is a measure of the width of the free-mixing zone. In the absence of experimental or theoretical information pertinent to nonsimilar and/or high-speed flows, this expression has been used as the basis for the forementioned models in the analysis of hypersonic wakes. However, the application to compressible flow requires the designation of the density on which the eddy diffusivity is based; hence, different expressions have evolved.

Model 1 has been assumed by Bloom and Steiger[8]; they assume that l is the transformed wake radius and that the wake axis density governs the turbulent transport. A value of $K = 0.02$ is taken as representative for incompressible jet and wake data.[21]

Model 2 is due to Ferri[44] and is based upon results of recent hydrogen-air supersonic combustion experiments. This model has been used successfully to explain the mixing of two streams of different composition but having identical velocities. A diffusivity based upon a velocity difference cannot be used to explain this type of mixing. The reference length l is interpreted by Ferri as a half-width (in the physical coordinates) based on ρU. A value of $K = 0.025$ has been used.

Model 3 has been derived by Ting and Libby[5, 45] on the basis of the transformation of the conservation equations to an equivalent incompressible system; i.e., with the Howarth transformation and model 3, the compressible conservation equations reduce to the incompressible equations. This

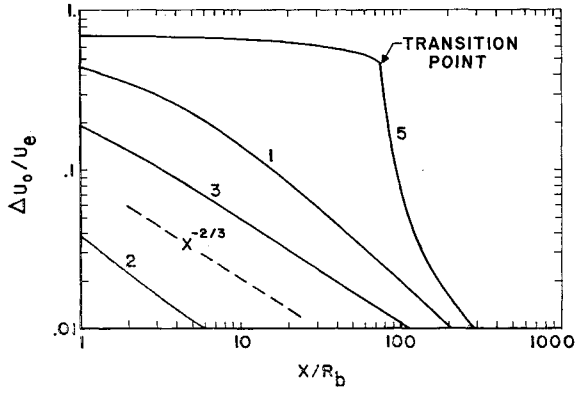

Fig. 7 Variation of axis velocity defect (10° cone, 120 kft, R_b = 1 ft). Turbulent and transition wakes.

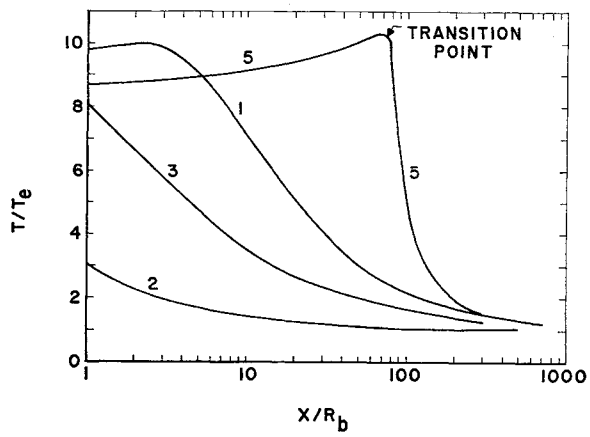

Fig. 8 Maximum wake temperature (10° cone, 120 kft, R_b = 1 ft). Turbulent and transition wakes.

model yields a compressible diffusivity that varies over the cross section and thus represents a departure from classical concepts.[21] A value of $K = 0.02$ has been used,[5] and l is taken to be the density transformed radius.

Model 4 has been derived by Lees and Hromas[2] based upon essentially the same arguments used by Ting and Libby, and, in fact, the result is the same as model 3 evaluated on the wake axis. Lees and Hromas deduce a value of $K \cong 0.04$ based on some of Townsend's data[43] and some of the details pertinent to their analysis.

In order to judge the quantitative effect of the viscosity model, wake calculations were performed using models 1, 2 and 3; model 4 was omitted because it is essentially the same as model 3, and thus wakes based on the two models show only minor quantitative differences (as indicated in Ref. 47). In these calculations, a value of $K = 0.04$ was used for all diffusivity models.¶ Additionally, a laminar-turbulent transition calculation was performed. The transition criterion is that presented by Pallone, et al.[13]; it is given in terms of a Reynolds number based on axis velocity defect and wake radius, and a Mach number based on axis velocity defect.** The diffusivity used in the turbulent portion of this calculation is model 1. The calculations apply to a 10° half-angle cone, having a base radius of 1 ft, flying with a velocity of 23,000 fps at 120 kft. The wake initial conditions were obtained by a chemically frozen streamtube expansion of the boundary layer at the shoulder of the cone to the freestream pressure (i.e., the wake was taken to be at constant pressure); the boundary layer was assumed to be laminar and in equilibrium. The stagnation-enthalpy profile was determined from a Crocco relation, with an axis value of 0.2 of the freestream value. (The reason for this relatively "cold" initial condition is that the calculations were taken from a parametric study.[46])

On Figs. 6–9, the curves marked 1, 2, and 3 correspond to viscosity models 1, 2, and 3; curve 5 is the laminar-turbulent transition calculation (model 1 in the turbulent region). The initial conditions show off-axis peaks in temperature and electron density; consequently, the maximum values of T and N_e- are shown in the figures. For the fully turbulent cases, the peak values are on the wake axis for $X/R_b > 2$, whereas for the laminar-turbulent transition case, the off-axis peaks persist for the entire laminar run.

Figures 6–9 show the streamwise variations of wake "velocity" radius, axis velocity defect, and maximum temperature and electron density. The "velocity" radius is de-

¶ This choice is arbitrary and was made for the purpose of using the same K for all calculations, thereby isolating the effect of the flow properties in the diffusivity model.

** More recent correlations[48, 49] based on freestream Reynolds and Mach numbers, achieve essentially the same results.

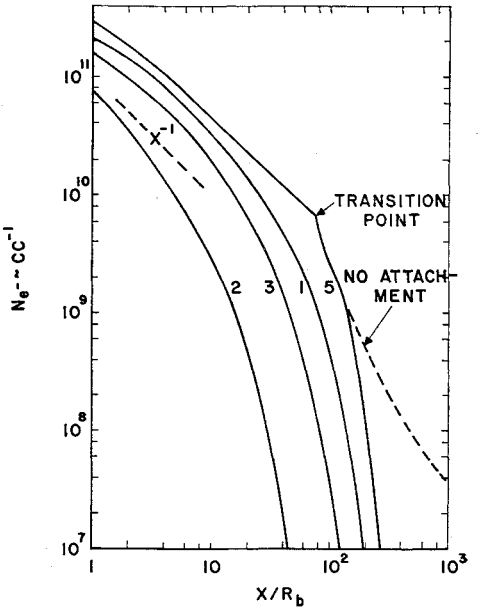

Fig. 9 Maximum wake electron density (10° cone, 120 kft, R_b = 1 ft). Turbulent and transition wakes.

fined as the radius at which the velocity defect is equal to 1% of the axis velocity defect.

The spread in the results obtained with the different models is in rough accord with the relative magnitudes of the viscosities. These relative magnitudes are, approximately, 1:100:10 for models 1, 2, and 3, respectively, in the present calculations, and it is seen that the X/R_b for the same level of a "diffusion-dominated" flow property (e.g., velocity) varies by a factor of about 50 from model 1 to model 2 and by a factor of about 3 from model 1 to model 3. However, for electron density, which is more "chemically controlled," the streamwise spread is substantially reduced; a factor of about 5 in X/R_b separates model 1 from model 2.

Models 2 and 3 result in the classical asymptotic behavior $\delta_U \sim X^{1/3}$ and $\Delta U_0 \sim X^{-2/3}$ for large X. However, model 1 yields $\delta_U \sim X^{1/2}$ and $\Delta U_0 \sim X^{-1}$ at large X since this viscosity is virtually constant, and thus there results a "laminar-type" decay.

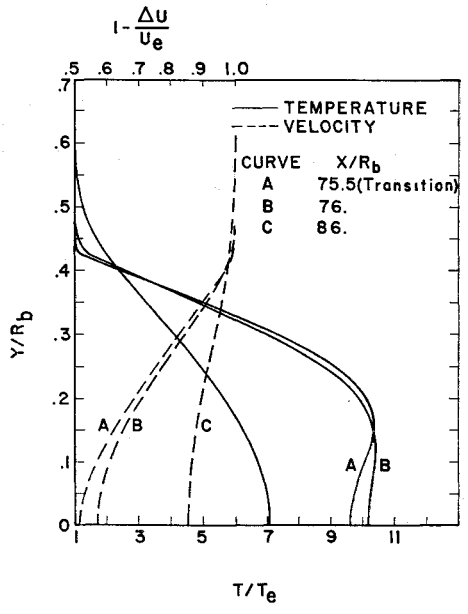

Fig. 10 Effect of transition on velocity and temperature profiles (10° cone, R_b = 1 ft, 120 kft). Model 1 diffusivity in turbulent region.

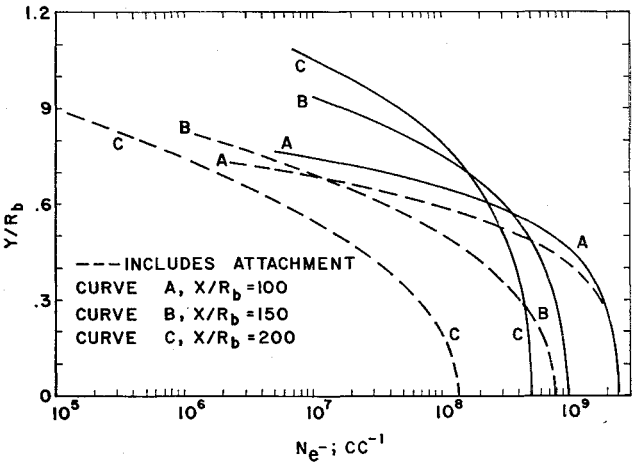

Fig. 11 Effect of O_2-electron attachment on electron density profiles (10° cone, R_b = 1 ft, 120 kft). Transition wake with model 1 diffusivity in turbulent region.

The transition calculation (curves 5) shows a rapid drive toward the corresponding all-turbulent case (curves 1 in this case) once transition takes place (X/R_b = 75.5). Figure 10 shows velocity and temperature profiles at the transition point and at two downstream stations. Marked changes of the laminar profiles are observed in a streamwise distance of 0.5 R_b.

The quantitative effects of the molecular oxygen-electron attachment process [reaction (6i)] are indicated for the transition wake in Figs. 9 and 11. The dashed line for curve 5 in Fig. 9 shows the decay of axis electron density resulting from recombination (and diffusion); an X^{-1} decay[11] is attained for large X. A comparison with the solid line, which includes attachment, shows the large effect of the attachment process in the downstream region (i.e., when, approximately, $T < 600$°K). For altitudes of about 150 kft and less, once it is initiated, the attachment reaction quickly approaches an equilibrium condition.[46]

Figure 11 shows electron density profiles with and without attachment effects. Since the attachment reaction is effective at low temperatures, it is first felt in the outer regions of the wake, as shown in Fig. 11. Further downstream, the "size" of ionized region is substantially reduced, e.g., at X/R_b = 200. The radii associated with 10^8 and 10^7 particles/cm^3 are reduced by factors of 4 and 2, respectively.

V. Summary

A finite-difference method has been employed to analyze the hypersonic wake with nonequilibrium air chemistry; both laminar and turbulent transport have been included.

Comparisons with an integral method[8] for a particular flight condition and laminar diffusion show large differences between the results of the two analyses.

Calculations for turbulent wakes with different turbulent diffusivity models show significant differences between these models. The differences appear to be large enough to detect experimentally; thus, suitably designed experiments could determine which model is more appropriate.

References

[1] Feldman, S., "On trails of axisymmetric hypersonic blunt bodies flying through the atmosphere," J. Aerospace Sci. **28**, 433–448 (1962).

[2] Lees, L. and Hromas, L., "Turbulent diffusion in the wake of a blunt-nosed body at hypersonic speeds," J. Aerospace Sci. **29**, 976–993 (1962).

[3] Long, M. E., "Hypersonic continuum wakes," General Electric Rept. GE TIS R605D440 (July 1961).

[4] Lenard, M., Long, M., and Wan, K. S., "Chemical non-equilibrium effects in hypersonic wakes," ARS Paper 2675-62 (1962).

[5] Ting, L. and Libby, P., "Fluid mechanics of axisymmetric wakes," General Applied Science Labs. Rept. GASL TR-145A (June 1960).

[6] Zeiberg, S. L., "Generalization of the oscillating wake analysis," General Applied Science Labs. Rept. GASL TR-307 (August 1962); also Proceedings of the 14th Semi-annual Meeting of Anti-Missile Research and Advisory Committee (S) (November 1962).

[7] Zeiberg, S. L., "The wake behind an oscillating vehicle," J. Aerospace Sci. **29**, 1344–1347 (1962).

[8] Bloom, M. H. and Steiger, M. H., "Diffusion and chemical relaxation in free mixing," IAS Paper 63-67 (1963).

[9] Lykoudis, P. S., "Ionization trails," *Proceedings of the 1961 Heat Transfer and Fluid Mechanics Institute* (Stanford University Press, Stanford, Calif., 1961), pp. 176–192.

[10] Wan, K. S., "A theory of laminar viscous wake for bodies at hypersonic speeds," IAS Summer Meeting, Los Angeles, Calif. (1962).

[11] Lees, L., "Hypersonic wakes and trails," ARS Paper 2662-62 (1962).

[12] Vaglio-Laurin, R. and Bloom, M. H., "Chemical effects in external hypersonic flows," *ARS Progress in Astronautics and Rocketry: Hypersonic Flow Research*, edited by F. R. Riddell (Academic Press, New York, 1962), Vol. 7, pp. 205–254.

[13] Pallone, A., Erdos, J., Eckerman, J., and McKay, W., "Hypersonic wakes and transition studies," AIAA Preprint 63-171 (1963).

[14] Lykoudis, P., "Laminar hypersonic trail in the expansion-conduction region," AIAA J. **1**, 772–775 (1963).

[15] Lykoudis, P., "The growth of the hypersonic turbulent wake behind blunt and slender bodies," Memo. RM-32-70-PR, Rand Corp. (January 1963).

[16] Hromas, L. and Lees, L., "Effect of nose bluntness on the turbulent hypersonic wake," Space Technology Labs., STL Rept. 6130-6259-RU-000 (October 1962).

[17] Klaimon, J. H., "The reentry wake in an earth fixed coordinate system," AIAA Preprint 63-185 (1963).

[18] Lien, H., Erdos, J., and Pallone, A., "Non-equilibrium wakes with laminar and turbulent transport," AIAA Preprint 63-447 (1963).

[19] Lin, S. C. and Hayes, J. E., "A quasi one-dimensional model for chemically reacting turbulent wakes of hypersonic objects," AIAA Paper 63-449 (1963).

[20] Webb, W. H. and Hromas, L. A., "Turbulent diffusion of a reacting wake," AIAA Preprint 64-42 (1964).

[21] Schlichting, H., *Boundary Layer Theory* (McGraw Hill Book Co., Inc., New York, 1955), Chap. 23.

[22] Dorodnitzin, A., "Method of integral relations for the numerical solution of partial differential equations," *Report of the Institute of Exact Mechanics and Computing Techniques* (Akademiya Nauk, USSR, 1958).

[23] Pallone, A., "Nonsimilar solutions of the compressible laminar boundary layer equations with applications to the upstream transpiration problem," J. Aerospace Sci. **28**, 450–456 (1959).

[24] Flugge-Lotz, I. and Baxter, D. C., "The solution of compressible laminar boundary layer problems by a finite difference method, Part I," Stanford Univ. TR-103 (September 1956).

[25] Flugge-Lotz, I. and Baxter, D. C., "The solution of compressible laminar boundary layer problems by a finite difference method, Part II," Stanford Univ. TR-110 (October 1957).

[26] Flugge-Lotz, I. and Blottner, F. G., "Computation of the compressible laminar boundary-layer flow including displacement thickness interaction using finite difference methods," Stanford Univ. TR-131 (January 1962).

[27] Kramer, R. F. and Lieberstein, H. M., "Numerical solution of the boundary layer equations without similarity assumptions," J. Aerospace Sci. **26**, 508–514 (1959).

[28] Wu, J. C., "The solution of laminar boundary layer equations by the finite difference method," *Proceedings of the 1961 Heat Transfer and Fluid Mechanics Institute* (Stanford University Press, Stanford, Calif., 1961), pp. 55–69.

[29] Howe, J. T., "Some finite difference solutions of the laminar compressible boundary layer showing the effects of upstream transpiration cooling," NASA Memo. 2-26-59A (February 1959).

[30] Der, J. and Raetz, G. S., "Solution of general three-dimensional boundary-layer problems by an exact numerical method," IAS Paper 62-70 (1962).

[31] Blottner, F. G., "Chemical non-equilibrium boundary layers," AIAA J. **2**, 232–239 (1964).

[32] Pai, S. I., "Axially symmetric jet mixing of a compressible fluid," Quart. Appl. Math **10**, 141–148 (1952).

[33] Vasilu, J., "Turbulent mixing of a rocket exhaust jet with a supersonic stream including chemical reactions," J. Aerospace Sci. **29**, 19–28 (1962).

[34] Howarth, L. (ed.), *Modern Developments in Fluid Dynamics* (Oxford University Press, London, 1953), Vols. 1 and 2, Chap. 10, Appendixes I and II.

[35] Lees, L., "Laminar heat transfer over blunt-nosed bodies at hypersonic flight speeds," Jet Propulsion **26**, 259–269 (1956).

[36] Teare, J. D. and Dreiss, G. J., "Theory of the shock front, III: Sensitivity to rate constants," Avco-Everett Research Lab., Res. Note 176 (December 1959).

[37] Nawrocki, P. J., "Reaction rates," Aerophysics Corp. of America, Rept. 61-2-A (1961).

[38] Chanin, L., Phelps, A., and Biondi, A., "Measurements of the attachment of low-energy electrons to oxygen molecules," Phys. Rev. **128**, 219 (1962).

[39] Richtmyer, R. D., *Difference Methods for Initial Value Problems* (Interscience Publishers, New York, 1957), Chaps. 1, 4, and 6.

[40] Southwell, R. V., *Relaxation Methods in Theoretical Physics* (Oxford University Press, New York, 1946), Chap. 1.

[41] Rossini, F. D. (ed.), *Thermodynamics and Physics of Matter, Vol. 1: High Speed Aerodynamics and Jet Propulsion* (Princeton University Press, Princeton, N. J., 1956), Chap. A1-4.

[42] Zeiberg, S. L. and Bleich, G. D., "A finite difference method solution of the laminar hypersonic non-equilibrium wake," General Applied Science Labs. Rept. GASL TR-338 (February 1963).

[43] Townsend, A. A., *The Structure of Turbulent Shear Flow* (Cambridge University Press, Cambridge, England, 1956), Chap. 7.

[44] Ferri, A., Libby, P. A., and Zakkay, V., "Theoretical and experimental investigation of supersonic combustion," Aeronautical Research Lab. Rept. 62-467 (September 1962).

[45] Ting, L. and Libby, P. A., "Remarks on the eddy viscosity in compressible mixing flows," J. Aerospace Sci. **27**, 797–798 (1960).

[46] Zeiberg, S. L., "Wake studies of oxygen-electron attachment and initial conditions," General Applied Science Labs. Rept. GASL TR-369 (January 1964); also "Oxygen-electron attachment in hypersonic wakes," AIAA J. **2**, 1151–1152 (1964).

[47] Zeiberg, S. L., and Bleich, G. D., "Finite difference calculation of hypersonic wakes," AIAA Preprint 63-448 (August 1963).

[48] Zeiberg, S. L., "Transition correlations for hypersonic wakes," AIAA J. **2**, 564–565 (1964).

[49] Levensteins, Z., "Hypersonic wake characteristics behind spheres and cones," AIAA J. **1**, 2848–2850 (1963).